Ubiquitous Fall Hazard Identification With Smart Insole

Diliang Chen , Golnoush Asaeikheybari , Huan Chen , Wenyao Xu , *Senior Member, IEEE*, and Ming-Chun Huang , *Member, IEEE*

Abstract—**Falls are leading causes of nonfatal injuries in workplaces which lead to substantial injury and economic consequences. To help avoid fall injuries, safety managers usually need to inspect working areas routinely. However, it is difficult for a limited number of safety managers to inspect fall hazards instantly especially in large workplaces. To address this problem, a novel fall hazard identification method is proposed in this paper which makes it possible for all workers to report the potential hazards automatically. This method is based on the fact that people use different gaits to get across different floor surfaces. Through analyzing gait patterns, potential fall hazards could be identified automatically. In this research, Smart Insole, an insole shaped wearable system for gait analysis, was applied to measure gait patterns for fall hazard identification. Slips and trips are the focus of this study since they are two main causes of falls in workplaces. Five effective gait features were extracted to train a Support Vector Machine (SVM) model for recognizing slip hazard, trip hazard, and safe floor surfaces. Experiment results showed that fall hazards could be recognized with high accuracy (98.1%).**

Index Terms—**Activity recognition, gait analysis, slips trips and falls (STF), smart insole, wearable healthcare.**

I. INTRODUCTION

FALLS on the same level is a serious problem with substantial injury and economic consequences. According to the 2018 Liberty Mutual Workplace Safety Index, falls rank second in the leading causes of nonfatal injuries in the workplace with direct costs of $11.2 billion and account for 19.2% of the total injury burden [1]. In addition, the number of fall cases causing sick days is increasing in major industries. According to the U.S. Bureau of Labor Statistics, the number of fall cases in the retail industry, which has the highest number of falls, increased to 34 190 cases in 2018, with an increase rate of 11% from 2017 [2].

To prevent falls and avoid fall injuries, the first step is to identify the fall hazards in a timely manner. The major causes of fall injuries lying on floors or ground surfaces including contaminated surfaces with water, oil, dust, extension cords, air hoses, and tools, etc. [3]. Asking safety managers to inspect working areas routinely is a popular method to recognize these hazards [4]. However, since these fall hazards could be created by any worker in the area, it is difficult for a limited number of safety managers to recognize hazards instantly [5]. In addition, people have different feelings on the safety of the same workplace because of differences in knowledge, skills, and age [5]–[7]. For instance, older workers might feel unsafe when walking on a surface, while younger workers might feel the surface is safe. A slightly uneven surface might cause imbalances and stumbles for elderly people but the surface could have been specified as safe through the current inspection methods [8].

To address these problems, we propose a novel method using Smart Insole as a medium to let all workers report potential fall hazards automatically. This method is based on the fact that people use different gaits to get across different surfaces or deal with different events that could lead to falls. When encountering slip or fall situations, people adjust their walking styles according to their prior experiences to maintain dynamic gait balance during locomotor activities (quantified by gait parameters) [9].

Therefore, through analyzing gait parameters, the condition of ground surfaces could be evaluated. In this research, Smart Insole was used for measuring gait parameters. Smart Insole is a wearable system that looks the same as a normal insole from the outside. To ensure a comprehensive gait analysis, an Inertial Measurement Unit (IMU) and an insole-shaped pressure sensor array with 96 pressure sensors were integrated into each Smart Insole. Our previous research had shown that the Smart Insole system could be used for measuring different kinds of gait parameters with high accuracy, including temporal gait parameters and force-related gait parameters [10], [11]. Since slips and trips are two main causes of falls in the workplace [12], recognizing fall hazards that could lead to slips and trips was the focus of this research. Contributions of this paper include:

1) Proposed a novel fall hazard identification method based on the fact that people use different gaits to get across ground surfaces with different hazards. This method makes it possible to recognize different types of fall

hazards automatically by analyzing the measured gait information.

2) Implemented the fall hazard identification method based on a low-cost and unobtrusive wearable system – Smart Insole, which makes it possible for all workers to report potential fall hazards automatically. Compared with the traditional fall hazard identification method which relies on safety managers, this automatic hazard identification method has the potential to increase efficiency and decrease costs.

3) Evaluated the method's performance in practice by introducing activities of daily living (ADLs), performed on safe floors, to the experiment. People use different gaits to perform different ADLs. Introducing ADLs performed on safe floors could help evaluate the performance of this method in discriminating safe floors and floors with fall hazards.

II. RELATED WORK

Falls in the workplace can be caused by risk factors such as small barriers, uneven surfaces, slippery surfaces, etc. In order to prevent consequent injuries, it is important to diminish hazards in the environment for all individuals [13]. Due to the importance of workplace safety and hazard identification, a lot of research has been done for increasing safety in the workplace. Maruyama *et al.* [13] proposed a new trip risk evaluation system. They detected potential hazards by creating a 3D simulation of a construction environment with laser-scanned point clouds. The interaction between a simulated digital human model (DHM) and the environment model develops an assessment value of the tripping risk of environment regions. This method is inefficient in dynamic ever-changing work environments. Yang *et al.* [14] proposed a hazard identification method based on the workers' moving trajectory. They assessed the degree of dissimilarity between the reference trajectory and the workers' trajectory. If the dissimilarity degree is larger than a certain number, there are some hazards in the region. The dissimilarity value is measured by the discrete Fréchet distance. However, this method is easy to give false alarms when people are taking a random walk in situations such as making a phone call.

Vision-based methods are also popular for hazard identification and safety management [15], [16]. However, these methods are costly because of the expense of cameras. In addition, the performance of these methods is also limited by environmental factors such as lighting conditions. For example, a slippery surface is hard to detect in a low light environment [17]. Han *et al.* [15] used computer vision technology to detect unsafe behaviors and improve workplace safety. Hazardous behaviors were detected by the identification of a 3D human skeleton. However, the performance of this method could be easily affected by various environmental visual occlusions. Kim *et al.* [18] developed a system that could inform users of hazardous situations in construction environments. They used a vision-based site monitoring module, a safety assessment module, and a visualization module. Identified hazards were augmented and displayed on a wearable device. This method could be negatively affected by environmental visual cues and the cost is high. With the advancements in wearable technologies, many wearable technologies have been developed for safety monitoring and hazard identification [19]. Bernal *et al.* [20] proposed a wearable vest system for industrial safety monitoring. The sensors for measuring vital signs such as respiration, heart rate, and galvanic skin response (GSR) were embedded in the vest. Furthermore, there was a force measurement platform embedded in the shoes which could vibrate if the user carries an excessive load. This platform could also inform the managers and nearby workers. The vibration would stop when the worker puts down the load. Yang *et al.* [17] proposed a method using a wearable inertial measurement unit (WIMU)–based Gait Abnormality Score (I-GAS) to indicate the existence of a fall hazard. However, this method cannot recognize the type of the detected hazard. Kim *et al.* [21] deployed WIMUs that could be attached to the human body and measure the workers' bodily response. The hazards in workplaces could be detected by analyzing bodily response data. Although the existence of fall hazards could be detected, the method cannot recognize the type of the detected hazard.

To address the aforementioned problems, we proposed a novel wearable method for fall hazard identification. Different from most of the methods which need multiple sensors to be positioned on different parts of the human body which make daily usage of the method obtrusive and uncomfortable [22], the method proposed in this paper used an unobtrusive wearable Smart Insole for data collection. Besides recognizing the existence of fall hazards, the types of hazards could also be recognized. In the following sections, system details and performance evaluation methods will be specified.

III. SYSTEM

The implementation of the fall hazard identification method proposed in this research relies on a wearable system for measuring gait parameters and an effective gait analysis method for hazard identification. In this section, the Smart Insole system for gait measurement, and the effective gait features for recognizing slip and trip hazards will be described.

A. Previous Work

1) Smart Insole: In this paper, Smart Insole was used to measure gait parameters. Fig. 1(a)–(c) shows the hardware system for data acquisition and wireless transmission and Fig. 1(d) shows the visualization effect of the plantar pressure on a smartphone application. Fig. 1(a) shows an insole-shape piezoresistive pressure sensors array. Ninety-six pressure sensors were uniformly distributed on the array, which ensures a high spatial resolution for measured plantar pressure. The pressure sensor array has a customizable design, which makes it possible to be trimmed to fit foot sizes from 5.5 US to 14 US [11], [23]. On the main circuit board shown in Fig. 1(b), an Inertial Measurement Unit (IMU) was used to measure the foot motion, a Flexible Printed Circuit (FPC) connector was used to connect the pressure sensor array with the circuit board, a Microcontroller Unit (MCU) was used to control the signal acquisition and processing, and a wireless transmission module was used for transferring data via Bluetooth. The data sampling frequency is 30 Hz. Fig. 1(c) shows the component structure of the Smart Insole. As shown in the figure, the Smart Insole uses a four-layer design. The first layer is a fabric layer for comfort. The second
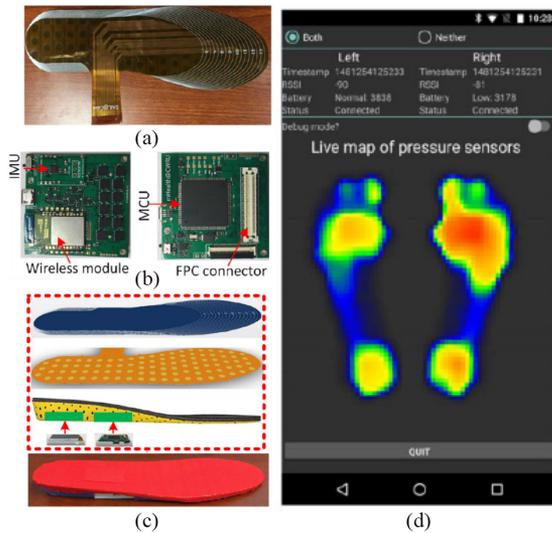
Fig. 1.   Smart Insole system design. (a) Insole shaped pressure sensor array; (b) main circuit board of the Smart Insole; (c) assembling structure of the Smart Insole. The first layer is a thin fabric layer to ensure wear comfort; the second layer is a pressure sensor array; the third layer is an insole shaped package; and the fourth layer consists of the main circuit board and a battery; (d) the smartphone application which could visualize the plantar pressure.

Fig. 2.   Gait characteristics for ADLs recognition. θ_{pitch} indicates the "foot contact pitch." Sub-figure (a)–(d) show the gait characteristics in "descending stairs," "walking," "ascending stairs," and "running," respectively.

layer is the pressure sensor array. The third layer is an insole shaped package. The circuit board ($46.1 \times 46.1 \times 6.2$ mm) and the Li-ion battery (3.7 V, 1000 mAh, $50.8 \times 33.5 \times 5.9$ mm) on the fourth layer were protected with 3D printed cases ($51.0 \times 51.0 \times 12.0$ mm and $60.0 \times 47.0 \times 11.0$ mm for the circuit board and battery, respectively) and embedded into the insole package. This unobtrusive design of the Smart insole makes it similar to a normal shoe. This feature makes Smart Insole an appropriate wearable system for daily usage in the workplace [10]. Fig. 1(d) shows the visualization of the plantar pressure on the smartphone application.

In our previous research [10], Smart Insole was used to measure 26 gait parameters, including temporal gait parameters, force related gait parameters, gait variability, gait symmetry, and turning related gait parameters. Since foot-contact and foot-off events could be detected correctly, errors of temporal gait parameters, such as gait cycle time and double support time, could be limited in one sampling period (i.e. 33 ms). For example, the error of the gait cycle time was 1.2 ± 14.9 ms [10]. Force related gait parameters were derived from Ground Reaction Force (GRF) which could be measured with high accuracy. Based on our previous research, the correlation of the GRF measured by Smart Insole and AMTI OR6 series force plate could reach 0.989 [10]. For measuring angles, the mean error was $1.93°$ when measuring a 180-degree turning [10]. In the following, the gait parameters measured by the Smart Insole will be analyzed to extract effective gait features for recognizing slip and trip hazards.

2) Safe Floor Activities: In practice, most of the floor surfaces are safe without slip and trip hazards. To design a method that could be used to discriminate safe floors and floors with fall hazards, activities of daily living (ADLs) including "walking," "running," "descending stairs," and "ascending stairs," performed on safe floors were also introduced.
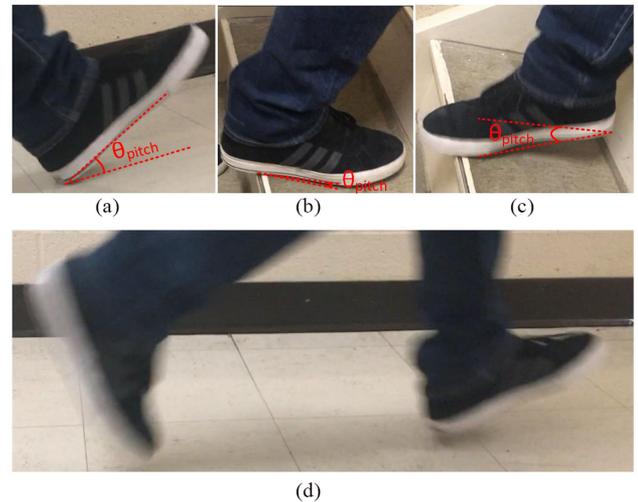
In our previous research, three features were used to recognize these four ADLs [10]. The first feature is "foot contact pitch" which is the pitch angle at the time when a foot initially contacts the ground. Fig. 2(a), (b), and (c) show the "foot contact pitch" of "descending stairs," "walking," and "ascending stairs" respectively. It is obvious that the "foot contact pitch" is larger than zero (i.e. the toe is higher than the heel) for "walking," around zero for "ascending stairs," lower than zero (i.e. the toe is lower than the heel) for "descending stairs." Therefore, based on this feature, "walking," "ascending stairs," and "descending stairs" could be discriminated. The second feature is the "percentage of double support time," which is the percentage of the double support time of the total gait cycle time. As shown in Fig. 2(d), for "running," the double support phase is replaced with the double float phase. Therefore, its "percentage of double support time" would be significantly lower than the other three activities. The third feature is the "foot contact pitch - GRF2 pitch." "GRF2 pitch" is the pitch angle at midstance. The "foot contact pitch - GRF2 pitch" is introduced to increase the classification reliability.

B. Slippery Surface Negotiation

Slippery surfaces are one of the main causes of fall injuries in the workplace. To prevent slipping and falling, people change their gait to maintain dynamic balance. Typical gait characteristics of walking on slippery surfaces include an increase in stride time and step-width as well as a decrease in stride length, walking speed, heel horizontal velocity, heel horizontal and vertical accelerations, loading speed on the supporting foot, and foot angle at heel contact etc. [24]–[31]. These adjustments to an individual's gait help reduce the chance of slipping and the severity of injuries that can occur from slipping. Taking the computation load and efficiency of the algorithms into consideration, the foot angle at heel contact (i.e. "foot contact pitch") was selected as one of the features for recognizing slippery surfaces. The decreased "foot contact pitch" leads to flat foot landing, which is one of the most important gait characteristics

Fig. 3. Details of trip negotiation to prevent fall. During the trip, the recovery limb (i.e. the right limb in the figure) would strike an unexpected obstacle. To prevent fall, the recovery limb would accelerate to pass over the obstacle. At the same time, the supporting limb (i.e. the left limb in the figure) would push the center of mass upwards to provide time and space for the placement of the recovery limb. The positions of the center of mass are indicated with white dots.

Fig. 4. Walking on a slippery surface. θ shows the foot contact pitch angle which is near zero when walking on a slippery surface.

for walking on slippery surfaces [32]–[34]. As shown in Fig. 4 the "foot contact pitch" is very small. However, the "ascending stairs" activity performed on safe surfaces also has a small "foot contact pitch" [10]. As a result, if relying solely on the "foot contact pitch," the "ascending stairs" activity performed on safe floors would be misclassified as the activity performed on slippery surfaces, which could lead to false alarms. Compared with the "ascending stairs" performed on safe floors, walking on slippery surface would have a decreased loading speed on the supporting foot. Therefore, to reduce the possibility of a false alarm, another feature for slippery surfaces recognition is based

on the loading speed on the supporting foot. In this research, the maximum loading speed on the supporting foot of each step (i.e. "Max GRF difference" shown in Table I) was extracted.

C. Trip Negotiation

In addition to slipping hazards, tripping hazards are also important factors that cause falls in the workplace. Workers might face elevation changes on the walking surfaces, such as trailing cables, unsuitable floor coverings, uneven or damaged floor surfaces, etc. All of these unpredicted obstacles could lead to falls, which generally occur when the swing foot strikes those obstacles [35], [36]. The striking event could significantly influence the pattern of the acceleration signal measured during the swing phase. Fig. 5 shows the method used to extract the difference in acceleration data patterns between normal steps and trip involved steps. The subfigure on the top shows GRF. Black dots indicate sample data points and red dots indicate the start and end of swing phases. Blue areas indicate swing phases and golden areas indicate stance phases. Swing and Stance phases were determined based on an adaptive threshold proposed in our previous research [10]. For a sample data, if its GRF is less than the adaptive threshold, then it will be recognized as a data sample in swing phases, if not, it will be recognized as a data sample in stance phases. The first sample of a swing phase is also the last sample of the previous stance phase, and the last sample of a swing phase is also the first sample of the following stance phase. Each step includes one swing phase and one stance phase. Therefore, in Fig. 5, there are three steps. The first and third steps are normal walking steps and the second step is a trip involved step. The figure on the bottom shows the acceleration magnitude. By comparing the acceleration data patterns of the swing phases of these three steps, it is obvious that the pattern of normal walking is simple – with the acceleration

TABLE I
GAIT FEATURES FOR FALL HAZARD IDENTIFICATION

| No.	Gait features	Description
1	Max GRF difference (in Body Weight (BW))	The maximum of the GRF difference between two successive data samples in one step.
2	Number of threshold crossing points	The number of crossing points between an experiential threshold and the acceleration magnitude signal in a swing phase.
3	Foot contact pitch (in degree)	The pitch angle at the time when foot initially contacts the ground.
4	Foot contact pitch-GRF2 pitch (in degree)	"GRF2 pitch" is the pitch angle at midstance. This feature is introduced to enhance the classification reliability.
5	Percentage of double support time	The percentage of double support time over the total gait cycle time.
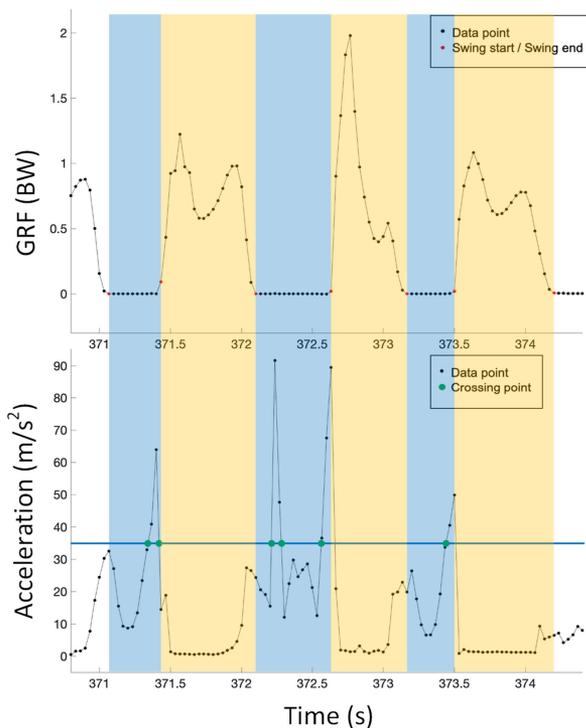
Fig. 5. Extracting the difference in acceleration data patterns between normal steps and trip involved steps. The first and third steps are normal walking steps and the second step is a trip step. The figure on the top shows the measured GRF. Black dots indicate sample data points and red dots indicate the start and end of swing phases. Blue areas indicate swing phases and golden areas indicate stance phases. The figure on the bottom shows the acceleration magnitude. The blue line indicates an empirical threshold of 35 m/s^2. Green dots indicate the crossing points between the threshold line and the acceleration magnitude curve in swing phases.

value decreased, then increased, and sometimes decreased again, but the pattern of the trip involved step is much more complex. To reflect this pattern difference, a feature named "number of threshold crossing points" was extracted. This feature indicates the number of crossing points between the acceleration data and an empirical threshold in the swing phase of a step. In this research, an empirical threshold of 35 m /s^2 was used. As shown in Fig. 5, there are one or two crossing points for normal walking steps but three crossing points for the trip involved step.

In addition to the feature that reflects the gait characteristic of the starting point of a trip event, another important feature related to the endpoint of a trip event was also extracted. In normal walking, a propelling momentum is created during push-off, and a countering force is created during the heel strike of the next step, which results in upright position maintenance. Successive positive and negative momentum cancel each other out and lead to continued walking activity. However, during a trip event, an external force is imposed on the body which leads to the forward rotation of the body and an increase in angular momentum. When trips occur, trip negotiation is needed to prevent the fall [37]. During trip negotiation, the gait pattern modifications often involve a rigorous reparameterization of forces within a short time frame [38]. As shown in Fig. 3, during the trip negotiation, the supporting limb propels the center of mass upwards then positions the pelvis forward, which provides the time and space for the appropriate placement of the recovery foot. Meanwhile, the recovery limb quickly passes over the obstacle with increased acceleration then immediately lowers to the floor in order to maintain balance and terminate the step before the fall. This causes a sudden increase in the GRF value. This gait characteristic makes the "Max GRF difference" higher during the trip steps. Therefore, the second feature for the trip hazard identification is the "Max GRF difference."

Finally, five features were extracted to recognize slipping and tripping hazards, and ADLs performed on safe floors. These five features were summarized in Table I. A support vector machine (SVM) was trained to recognize fall hazards and ADLs.

IV. EXPERIMENTS AND RESULTS

In this section, experiments were designed to evaluate the performance of the proposed method in fall hazard identification.

A. Data Collection

As described in Section III, five features were extracted to train a SVM model for recognizing fall hazards and the ADLs performed on safe floors. To avoid overfitting of the model on one subject, 10 subjects were involved in the experiment. During the experiment, each subject wore a pair of Smart Insole for data recording and performed each activity according to instructions.

	Predicted Class						
	Safe floor						
	Walking	Running	Descending stairs	Ascending stairs	Slip hazard	Trip hazard	Recall
Walking	297				1	2	99.0%
Running	1	294			1	4	98.0%
Descending stairs			298	1		1	99.3%
Ascending stairs				293	6	1	97.7%
Slip hazard	1			6	293		97.7%
Trip hazard	6	3				291	97.0%
Precision	97.4%	99.0%	100%	97.7%	97.3%	97.3%	98.1%

(Actual Class — Safe floor labels on left margin)

Fig. 6. Confusion matrix of the trained quadratic SVM model for safe floor activities and fall hazard identification.

For "walking" and "running," the subjects performed each activity 3 times along a straight hallway of 30 m long. For "descending stairs" and "ascending stairs," the subjects performed each activity 10 times along a stair with 9 steps. For walking on a "slippery surface," the subjects walked along a straight slippery path of 4 m long 10 times. The "slip hazard" was created by spraying detergent on a mosaic tiled surface. "Trip hazard" was created by using a fixed box of 14 cm heights, consistent with previous trip studies that used obstacles with 10-15 cm heights [32], [39], [40]. It created an elevated surface on the walking path. During the experiment, the subjects were tripped without falling 30 times. All the subjects used their comfort gait to perform different activities. To balance the training dataset, for each activity of each subject, 30 steps were used for feature extraction. Finally, there were 300 samples in the dataset for each activity. 5-fold cross-validation is used to evaluate the performance of the SVM classification model.

B. Results

Signal processing was performed on Matlab (MathWorks, Inc.). Fig. 6 shows the confusion matrix of the SVM model with quadratic kernel for safe floor activities and fall hazard identification. The overall accuracy is 98.1%. For ADLs performed on safe floors, the recall values are 99.0%, 98.0%, 99.3%, and 97.7% for "walking," "running," "descending stairs," and "ascending stairs," respectively. For identifying slip hazard and trip hazard, the recall values could reach 97.7% and 97.0%, respectively. This result indicates that with these five features, the proposed method could identify fall hazards and safe floor activities with high accuracy.

In this research, two features were extracted to identify each fall hazard: "Max GRF difference" and "foot contact pitch" were extracted for identifying slip hazard, and "Max GRF difference" and "number of threshold crossing points" were used for identifying trip hazard. To have a further understanding of the contribution of each feature combinations in identifying
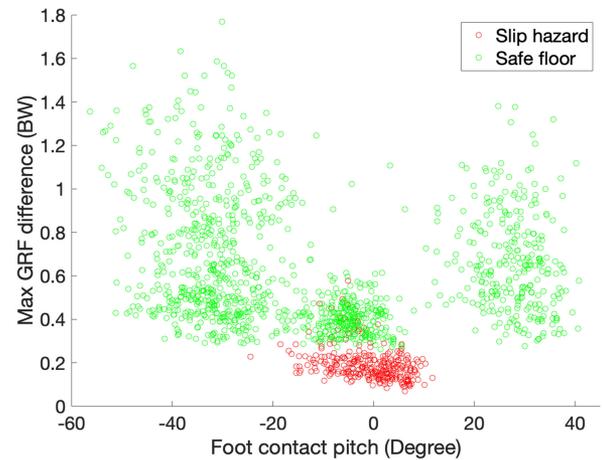

Fig. 7. Distribution of slip hazard and safe floor activities in the space defined by "Max GRF difference" and "Foot contact pitch." Green circles indicate the data samples of safe floor activities, including "walking," "running," "descending stairs," and "ascending stairs"; Red circles indicate the data samples of the walking activity performed on the floor with slip hazards.
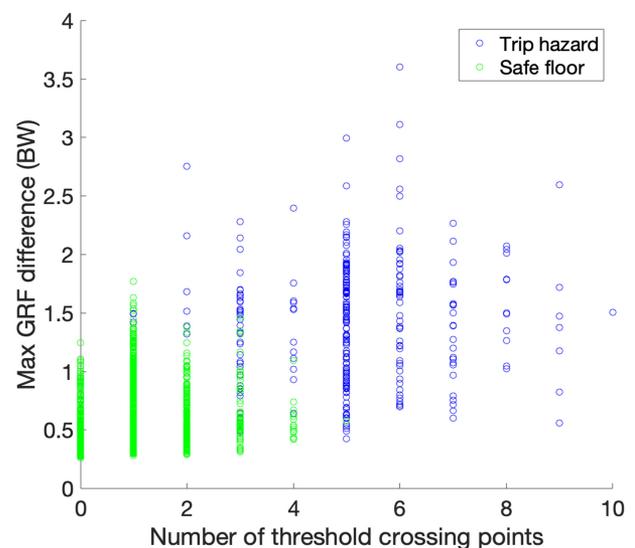

Fig. 8. Distribution of trip hazard and safe floor activities in the space defined by "Max GRF difference" and "number of threshold crossing points." Green circles indicate the data samples of safe floor activities. Blue circles indicate the data samples of activities performed during trip negotiation.

the corresponding fall hazard, the performance of these feature combinations were analyzed separately.

1) Performance of the Features for Slip Hazard Identification: Fig. 7 shows the distribution of safe floors activities (green circles) and the walking activity performed on slippery floors (red circles) in the space defined by "Max GRF difference" and "foot contact pitch." It is obvious that most of the data samples could be correctly separated into different groups only with these two features. This result indicates that these two features have a good performance in identifying slip hazards.

2) Performance of the Features for Trip Hazard Identification: Fig. 8 shows the distribution of safe floors activities (green
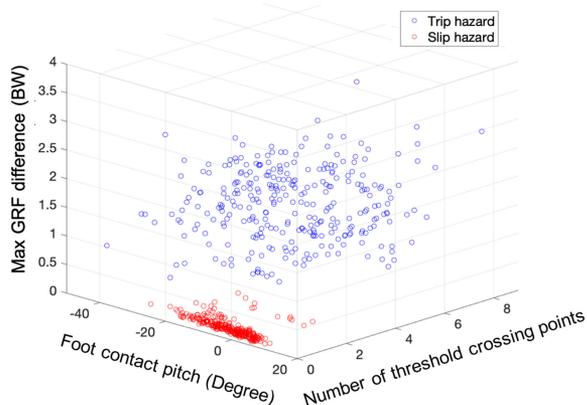
Fig. 9. Distribution of slip hazard and trip hazard in the space defined by "Max GRF difference," "Foot contact pitch," and "Number of threshold crossing points." Red circles indicate the data samples of walking activity performed on the floor with slip hazards; Blue circles indicate the data samples of activities performed during trip negotiation.

circles) and the trip negotiation activity (blue circles) in the space defined by "Max GRF difference" and "number of threshold crossing points." As shown in the figure, most of the data samples could be correctly separated into different groups. This result indicates that these two features have a good performance in identifying the trip hazard.

3) Performance of the Features for Discriminating Slip and Trip Hazard: Until now, experiment results have shown that the combination of "Max GRF difference" and "foot contact pitch" could discriminate safe floors and slip hazard, and the combination of "Max GRF difference" and "number of threshold crossing points" could discriminate safe floors and trip hazard. To get a further understanding of the contribution of these features in discriminating slip hazard and trip hazard, further analysis is necessary. Fig. 9 shows the distribution of the walking activity performed on slippery floors (red circles) and the trip negotiation activity (blue circles) in the space defined by "Max GRF difference," "foot contact pitch," and "number of threshold crossing points." As shown in the figure, these two fall hazards could be correctly separated into different groups. This result indicates that these three features have a good performance in discriminating different fall hazards in practice.

Finally, the experiment results indicate that (1) those five features have a good performance in identifying safe floors and the floor with fall hazards (i.e. slip hazard and trip hazard); (2) those specific feature combinations have a good performance in identifying the corresponding fall hazards.

V. DISCUSSION

In this section, some further findings and limitations of the proposed method will be discussed.

A. Personalized Classification Model Will Be Helpful to Improve the Accuracy of Fall Hazard Identification

To evaluate the generalization performance of the fall hazard identification method across subjects, 5-fold cross-validation was done in terms of different subjects. In this experiment, ten subjects were randomly split into five groups. For each test,

TABLE II
GENERALIZATION PERFORMANCE ACROSS SUBJECTS

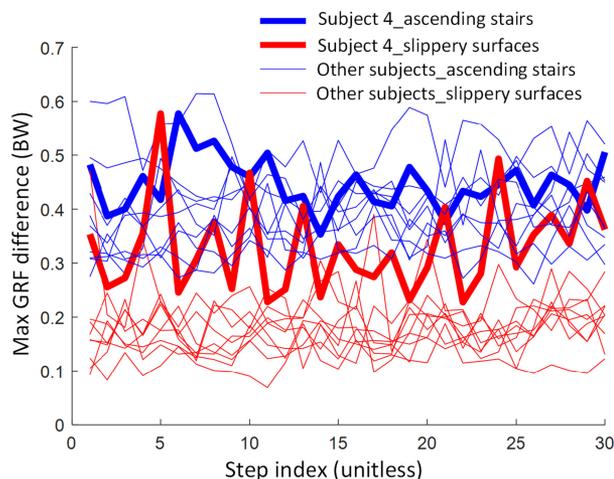|	Fold 1	Fold 2	Fold 3	Fold 4	Fold 5	Mean
Accuracy (%)	97.5	93.89	95.28	98.61	93.61	95.78

Fig. 10. Max GRF difference of all the 10 subjects during activities of ascending stairs and walking on slippery surfaces. The thick blue line and thick red line indicate the Max GRF difference of subject 4 during ascending stairs and walking on slippery surfaces, respectively. Thin blue lines and thin red lines indicate the Max GRF difference of the other 9 subjects during ascending stairs and walking on slippery surfaces, respectively.

the data of four groups of subjects was used for model training and the data of the remaining one group of subjects was used for testing. As shown in Table II, test accuracy from fold 1 to fold 5 were 97.5%, 93.89%, 95.28%, 98.61%, and 93.61%, respectively, and the mean accuracy was 95.78%.

Compared with the result shown in Fig. 6, there are some variations in the accuracy. These variations were caused by the fact that for the 5-fold cross-validation in terms of different subjects, the trained classification model was not able to include some special characteristics in the data of new testing subjects while the subjects were not in the training set. For example, the decrease in the accuracy of test 2 was mainly caused by misclassifications between "ascending stairs" and "slippery hazard" for the data of subject 4, who was one of the two testing subjects in fold 2. The reason for these misclassifications was that the "Max GRF difference" data of subject 4 during walking on slippery surfaces were much higher than that of the other subjects but the trained classification model in fold 2 was not able to take this characteristic into consideration. Fig. 10 shows the "Max GRF difference" of all the ten subjects during activities of ascending stairs and walking on slippery surfaces. Thin blue lines and thin red lines indicate the "Max GRF difference" of nine subjects (not including subject 4) during ascending stairs and walking on slippery surfaces, respectively. Through comparing blue and red thin lines, it is obvious that most of the "Max GRF difference" data during ascending stairs are larger than walking on slippery surfaces. However, as shown in the thick red line, the "Max GRF difference" of subject 4 during walking on slippery surfaces is much larger than the other subjects. Therefore, without taking

this special data characteristic of subject 4 into consideration, it will be difficult for the trained model to achieve a good performance.

The thick blue line shows the "Max GRF difference" of subject 4 during ascending stairs. Through comparing blue and red thick lines, it is obvious that most of the "Max GRF difference" during ascending stairs are still larger than walking on slippery surfaces. This means that subject 4 still used a decreased loading speed on the supporting foot as expected when walking on slippery surfaces although his degree of decrease was not as obvious as other subjects. Therefore, to increase the classification performance of the proposed method, personalized training models, which can take personalized gait features into consideration, will be explored in the future.

B. Feature Evaluation

Using minimum redundancy - maximum relevance (MRMR), the features were ranked as follows: foot contact pitch, max GRF difference, percentage of double support time, foot contact pitch-GRF2 pitch, and the number of thresholds crossing points. We repeated the classification while sequentially adding the features based on their ranking and evaluated classifier accuracy with each incremental change in features in a five-fold cross-validation setting. The results showed that accuracy increased continuously from 39.54% (one feature) to 95.78% (five features). This result indicates that using five features leads to the best overall accuracy in classification.

C. Two Different Trip Negotiation Strategies

Based on the previous researches [41], the reaction of people in restraining the momentum in the trip recovery phase mostly falls into two groups. In the first group, during the push-off, the angular momentum decreases and the forward rotation that body obtains due to the trip impact has been totally eradicated. Therefore, the subject could regain normal walking after one step of the recovery foot. In the second group, the subject can terminate the elevation of angular momentum but cannot decrease the momentum. Therefore, one extra step of the recovery foot is required to completely dispel the forward rotation of the body. Fig. 11 uses GRF recorded during three repetitions of the trip experiment to show each trip negotiation strategy. As shown in Fig. 11(a), there is only one step for the first kind of trip negotiation. As shown in Fig. 11(b), for the second kind of trip negotiation, there are two steps. For both of the trip negotiation strategies, the proposed method could identify the trip hazard based on the extracted gait features.

D. Combination With Indoor Localization Function

In our previous research, we proposed an indoor localization method based on Smart Insole [23]. Combining the indoor localization approach and the fall hazard detection system, the Smart Insole system has the potential to supply not only the type of fall hazards but also the location of the detected hazards. This information will help improve the efficiency of safety managers in removing potential fall hazards.
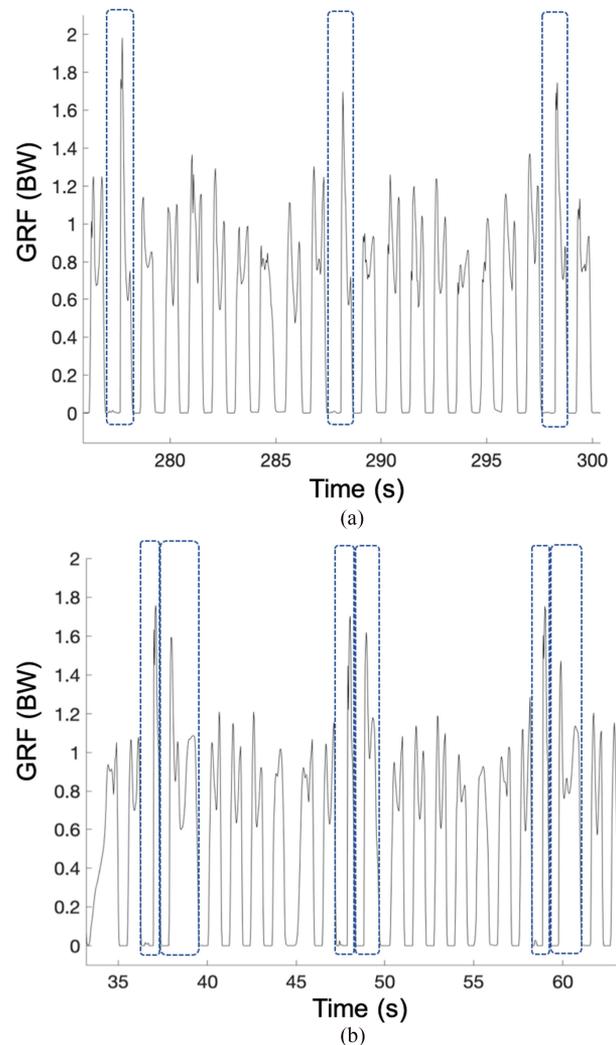

Fig. 11. Two major types of trip negotiation method. Dashed rectangles are used to indicate the GRF related to trip negotiation steps. (a) The first group of trip negotiation, during which the trip momentum is eradicated in one step. Therefore, there is one step during the trip negotiation. (b) The second group of trip negotiation, during which two steps are needed to restrain the momentum and prevent the fall.

E. Limitations of This Research

In this research, four different ADLs (i.e. "walking," "running," "descending stairs," "ascending stairs") performed on safe floors were introduced into the experiment to simulate real-world conditions. And the experiment results showed that the proposed method could discriminate fall hazards and safe-floor activities with high accuracy. However, those four ADLs cannot represent all the complex conditions (e.g. different working activities, distracted/dual-task conditions, different working environments, dark conditions in which people do not adjust their gates, etc.) in the real-world. To apply the proposed method in a real-world workplace, different parameters (e.g. the empirical threshold for calculating the "number of threshold crossing points") and new gait features might need to be explored based on specific applications.

In addition, only healthy subjects were involved in this research. In the future work, we will consider other types of

subjects in real-world conditions such as patients with stroke and disability, soldiers who may have a heavy load on the body which may change their balance and walking styles.

VI. CONCLUSION

In this paper, a novel wearable solution for fall hazard identification was proposed. This solution is based on the fact that people use different gaits to get across different floors. Implemented of this solution was based on a wearable gait analysis system – Smart Insole which made it possible for all the workers to report the potential hazards automatically. The experiment results showed that the proposed method could recognize ADLs performed on safe floors, slip hazard, and trip hazard with an overall accuracy of 98.1%. This result indicates that the proposed method has the potential to be used for fall hazard identification.

REFERENCES

[1] Liberty Mutual Insurance, *Liberty Mutual Workplace Safety Index*, 2018. [Online]. Available: https://business.libertymutualgroup.com/business-insurance/Documents/Service s/Workplace%20Safety%20Index.pdf

[2] US Department of Labor US Bureau of Labor Statistics. Employer-reported workplace injuries and illnesses, US Department of Labor, 2018.

[3] H. T. Yeoh, T. E. Lockhart, and X. Wu, "Non-fatal occupational falls on the same level," *Ergonomics*, vol. 56, no. 2, pp. 153–165, 2013.

[4] W.-R. Chang, S. Leclercq, T. E. Lockhart, and R. Haslam, "State of science: Occupational slips, trips and falls on the same level," *Ergonomics*, vol. 59, no. 7, pp. 861–883, 2016.

[5] S. Bahn, "Workplace hazard identification and management: The case of an underground mining operation," *Saf. Sci.*, vol. 57, pp. 129–137, 2013.

[6] G. Carter and S. D. Smith, "Safety hazard identification on construction projects," *J. Constr. Eng. Manage.*, vol. 132, no. 2, pp. 197–205, 2006.

[7] H. H. Cohen, and D. M. Cohen, "Psychophysical assessment of the perceived slipperiness of floor tile surfaces in a laboratory setting." *J. Saf. Res.*, vol. 25, no. 1, pp. 19–26, 1994.

[8] A. Ståhl, G. Carlsson, P. Hovbrandt, and S. Iwarsson, "let's go for a walk: Identification and prioritisation of accessibility and safety measures involving elderly people in a residential area," *Eur. J. Ageing*, vol. 5, no. 3, pp. 265–273, 2008.

[9] T. Lockhart, "Biomechanics of human gait-slip and fall analysis," in *Encyclopedia of Forensic Sciences*, 2nd ed., Elsevier Inc., New York, USA, 2012, pp. 466–476.

[10] D. Chen *et al.*, "Bring gait lab to everyday life: Gait analysis in terms of activities of daily living," *IEEE Internet Things J.*, vol. 7, no. 2, pp. 1298–1312, Feb. 2020.

[11] D. Chen, Y. Cai, and M.-C. Huang, "Customizable pressure sensor array: Design and evaluation," *IEEE Sensors J.*, vol. 18, no. 15, pp. 6337–6344, 2018.

[12] X. Dong, X. Wang, and R. Katz, "The Construction Chart Book . The U.S. Construction Industry and Its Workers," 6th ed., *CPWR . The Center for Construction Research and Training*, Maryland, USA, 2018.

[13] T. Maruyama, S. Kanai, and H. Date, "Tripping risk evaluation system based on human behavior simulation in laser-scanned 3d as-is environments," *Autom. Constr.*, vol. 85, pp. 193–208, 2018.

[14] K. Yang, C. R. Ahn, and H. Kim, "Tracking divergence in workers' trajectory patterns for hazard sensing in construction," *Constr. Res. Congr.*, pp. 126–133, 2018.

[15] S. Han and S.H. Lee, "A vision-based motion capture and recognition framework for behavior-based safety management," *Autom. Constr.*, vol. 35, pp. 131–141, 2013.

[16] M.-W. Park, N. Elsafty, and Z. Zhu, "Hardhat-wearing detection for enhancing on-site safety of construction workers," *J. Constr. Eng. Manage.*, vol. 141, no. 9, 2015, Art. no. 0 4015024.

[17] K. Yang, C. R. Ahn, M. C. Vuran, and H. Kim, "Sensing workers gait abnormality for safety hazard identification," in *Proc. 33rd Int. Symp. Autom. Robot. Constr.*, vol. 33, 2016.

[18] K. Kim, H. Kim, and H. Kim, "Image-based construction hazard avoidance system using augmented reality in wearable device," *Autom. Constr.*, vol. 83, pp. 390–403, 2017.

[19] K. Yang, C. R. Ahn, M. C. Vuran, and H. Kim, "Collective sensing of workers' gait patterns to identify fall hazards in construction," *Autom. Constr.*, vol. 82, pp. 166–178, 2017.

[20] G. Bernal, S. Colombo, A. M.A. Baky, and F. Casalegno, "Safety++: Designing IoT and wearable systems for industrial safety through a user centered design approach," in *Proc. 10th Int. Conf. Pervasive Technol. Related Assistive Environ.*, pp. 163–170, 2017.

[21] H. Kim, C. R. Ahn, and K. Yang, "Identifying safety hazards using collective bodily responses of workers," *J. Constr. Eng. Manage.*, vol. 143 no. 2, 2017, Art. no. 04016090.

[22] E. S. Sazonov, G. Fulk, J. Hill, Y. Schutz, and R. Browning, "Monitoring of posture allocations and activities by a shoe-based wearable sensor," *IEEE Trans. Biomed. Eng.*, vol. 58, no. 4, pp. 983–990, 2010.

[23] D. Chen *et al.*, "Smart insole-based indoor localization system for Internet of Things applications," *IEEE Internet. Things J.*, vol. 6, no. 4, pp. 7253–7265, 2019.

[24] R. Cham, B. Moyer, and M. S. Redfern, "Effect of having a-priori knowledge of the floor's contaminant condition on the biomechanics of slips," in *Proc. Hum. Factors Ergonom. Soc. Annu. Meeting*, vol. 46, no. 3, pp. 1181–1185, 2002.

[25] E. E. Swensen, J. L. Purswell, R. E. Schlegel, and R. L. Stanevich, "Co-efficient of friction and subjective assessment of slippery work surfaces," *Hum. Factors*, vol. 34, no. 1, pp. 67–77, 1992.

[26] Y. Bunterngchit, T. Lockhart, J. C. Woldstad, and J. L. Smith, "Age related effects of transitional floor surfaces and obstruction of view on gait characteristics related to slips and falls," *Int. J. Ind. Ergonom.*, vol. 25, no. 3, pp. 223–232, 2000.

[27] D. T.-P. Fong, Y. Hong, and J. X. Li, "Lower-extremity gait kinematics on slippery surfaces in construction worksites," *Med. Sci. Sports Exerc.*, vol. 37, no. 3, pp. 447–454, 2005.

[28] T. E. Lockhart, J. M. Spaulding, and S. H.Park, "Age-related slip avoidance strategy while walking over a known slippery floor surface," *Gait Posture*, vol. 26, no. 1, pp. 142–149, 2007.

[29] Jasmine C. Menant, Julie R. Steele, Hylton B. Menz, Bridget J. Munro, and Stephen R. Lord, "Effects of walking surfaces and footwear on temporo-spatial gait parameters in young and older people," *Gait Posture*, vol. 29, no. 3, pp. 392–397, 2009.

[30] G. Cappellini, Y. P Ivanenko, N. Dominici, R. E Poppele, and F. Lacquaniti, "Motor patterns during walking on a slippery walkway," *J. Neurophysiol.*, vol. 103, no. 2, pp. 746–760, 2010.

[31] R. Cham and M. S. Redfern, "Changes in gait when anticipating slippery floors," *Gait Posture*, vol. 15, no. 2, pp. 159–171, 2002.

[32] Y. Okubo *et al.*, "Exposure to trips and slips with increasing unpredictability while walking can improve balance recovery responses with minimum predictive gait alterations," *PLoS One*, vol. 13 no. 9, 2018, Art. no. e0202913.

[33] T. Bhatt, JD Wening, and Y.-C. Pai, "Adaptive control of gait stability in reducing slip-related backward loss of balance," *Exp. Brain Res.*, vol. 170, no. 1, pp. 61–73, 2006.

[34] T.-Y. Wang, T. Bhatt, F. Yang, and Y.-C. Pai, "Generalization of motor adaptation to repeated-slip perturbation across tasks," *Neuroscience*, vol. 180, pp. 85–95, 2011.

[35] A. Merryweather, B. Yoo, and D. Bloswick, "Gait characteristics associated with trip-induced falls on level and sloped irregular surfaces," *Minerals*, vol. 1, no. 1, pp. 109–121, 2011.

[36] M. Pijnappels, M. F. Bobbert, and J. H. van Dieën, "Changes in walking pattern caused by the possibility of a tripping reaction," *Gait Posture*, vol. 14, no. 1, pp. 11–18, 2001.

[37] T. J. Ayres and R. Kelkar, "Sidewalk potential trip points: A method for characterizing walkways," *Int. J. Ind. Ergonom.*, vol. 36, no. 12, pp. 1031–1035, 2006.

[38] A. R. DenOtter, A. C. H Geurts, M. DeHaart, T. Mulder, and J. Duysens, "Step characteristics during obstacle avoidance in hemiplegic stroke," *Exp. Brain Res.*, vol. 161, no. 2, pp. 180–192, 2005.

[39] T.-Y. Wang, T. Bhatt, F. Yang, and Y.-C. Pai, "Adaptive control reduces trip-induced forward gait instability among young adults," *J. Biomech.*, vol. 45, no. 7, pp. 1169–1175, 2012.

[40] M. Pijnappels, M. F. Bobbert, and J. H. van Dieën, "How early reactions in the support limb contribute to balance recovery after tripping," *J. Biomech.*, vol. 38, no. 3, pp. 627–634, 2005.

[41] M. Pijnappels, M. F. Bobbert, and J. H. van Dieën, "Contribution of the support limb in control of angular momentum after tripping," vol. 37, no. 12, pp. 1811–1818, 2004.